Metastable diamagnetic response of 20 nm $La_{1-x}MnO_3$ particles

V. Markovich,[1,*] I. Fita,[2,3] A. Wisniewski,[2] R. Puzniak,[2] D. Mogilyansky,[4] L. Titelman,[4] L. Vradman,[4] M. Herskowitz,[5] and G. Gorodetsky[1]

[1]*Department of Physics, Ben-Gurion University of the Negev, 84105 Beer-Sheva, Israel*
[2]*Institute of Physics, Polish Academy of Sciences, Aleja Lotnikow 32/46, 02-668 Warsaw, Poland*
[3]*Donetsk Institute for Physics & Technology, National Academy of Sciences, 83114 Donetsk, Ukraine*
[4]*Department of Chemical Engineering, Sami Shamoon College of Engineering, 84100 Beer-Sheva, Israel*
[5]*Blechner Center for Industrial Catalysis & Process Development, Department of Chemical Engineering, Ben-Gurion University of the Negev, 84105 Beer-Sheva, Israel*

(Received 8 April 2007; revised manuscript received 17 June 2007; published 16 January 2008)

The magnetic properties of compacted 20 nm $La_{1-x}MnO_3$ particles, prepared by the citrate method, in pristine and metastable states have been investigated. It was found that in its pristine state the investigated sample displays a paramagnetic-to-ferromagnetic transition near $T_C \approx 220$ K, below which the relative volume of the ferromagnetic (FM) phase at 5 K approaches a value of about 24%. Magnetization and ac-susceptibility measurements exhibit a cluster-glass-like behavior characterized by a noticeable difference between zero-field-cooled and field-cooled magnetization and frequency-dependent ac susceptibility. Different metastable states with highly reduced FM phase and "negative ferromagnetism" developed after a series of quick coolings of the sample placed in a container filled with silicon oil. The recorded temperature dependence of the negative FM moment appears to be a normalized replica of the corresponding FM dependence. Hysteresis loops of magnetization at low temperatures in both pristine and diamagnetic (DIA) states exhibit the same value of coercive field at 5 K, $H_C \approx 400$ Oe. The abnormal DIA state can only be erased after a few hours storage of the sample at room temperature. These observations are discussed with reference to a model in which the negative ferromagnetism is attributed to the appearance of nondispersive orbital currents which result in a coupling between the core of the FM particles and the surrounding diamagnetic matrix formed during the quick cooling cycles.

DOI: 10.1103/PhysRevB.77.014423 PACS number(s): 75.47.Lx, 75.50.Tt, 75.20.−g

I. INTRODUCTION

In recent years, anomalous diamagnetism and negative magnetization were reported for various perovskite structures.[1–8] Different scenarios were proposed to tackle this abnormal behavior: (i) a structural phase transition leading to a reversal of the Dzyaloshinskii vector;[1,2] (ii) a negative coupling between sublattices of 3*d* and 4*f* ions, leading to a sort of ferrimagnetism;[3–7] (iii) a change of sign in the *d-f* exchange interactions.[8] It is well known that Dzyaloshinskii-Moriya antisymmetric exchange[9,10] is responsible for slight canting of the spins of antiferromagnetic (AFM) sublattices, resulting in a weak ferromagnetic (FM) component (Dzyaloshinskii vector). Usually, this weak FM moment is equal to $10^{-2}-10^{-5}$ of the maximal magnetization of the nominal magnetic moments. Since "anomalous diamagnetism" in perovskite orthovanadates was attributed to reversal of the Dzyaloshinskii vector,[1,2] the negative magnetization observed in these compounds was relatively small, less than 10^{-2} emu/g.[1,2] Negative magnetization was observed also in some manganites, such as $(Dy,Ca)MnO_3$,[3,4] $Gd_{0.67}Ca_{0.33}MnO_3$,[5] $La_{1-x}Gd_xMnO_3$,[6] $NdMnO_{3+\delta}$,[7] $Nd_{1-x}Ca_xMnO_y$,[8] and $(Nd,Ca)(Mn,Cr)O_3$.[8] The reversal of magnetization in these compounds was attributed to a ferrimagneticlike behavior due to the interplay of two antiferromagnetically coupled magnetic sublattices: the rare-earth sublattice and the Mn sublattice. If the magnetizations of the two sublattices have different temperature dependences and, at decreasing temperature, the magnetization of the sublattice aligned antiparallel with the magnetic field (rare-earth sublattice) increases more rapidly than that aligned with the field, the net moment may point opposite to the applied magnetic field in a ferrimagneticlike state below the compensation temperature (T_{comp}). It should be noted that the magnetization vs field dependences in all the above compounds becomes positive at modest magnetic fields of a few hundreds of oersteds.

In this paper, we present experimental observations of diamagnetism and "negative ferromagnetism" in compacted 20 nm $La_{1-x}MnO_3$ nanoparticles, induced by quick cooling of a sample placed in a container filled with silicon oil. It was found that the sample retains these features at relatively high magnetic fields and at all temperatures below T_C. Since the temperature dependence of compacted 20 nm $La_{1-x}MnO_3$ nanoparticles exhibits only a single magnetic transition and quite unusual $M(H)$ dependence (the negative mangnetization increases monotonically with increasing magnetic field), we believe that none of the above scenarios are applicable here. For further discussion we refer to Troyanchuk *et al.*[8] and our[11] recent publications.

Several attempts have been made recently to establish a quantitative model that will account for the abnormal diamagnetism and reversed magnetization. Mattis[12] reported model calculations of electrons confined to the conduction band of an intrinsic semiconductor that is cut up into various nanoarchitectures. Taking into account the Coulomb interaction, he found that the ground state favors an AFM phase, a FM phase, and, ultimately, a superconducting phase, depend-

ing on electron concentration ν.[12] In particular, for the antidot lattice he found that at $\nu=1$ electron per nanocell the insulating phase is antiferromagnetic, while high-T_C-like superconductivity is expected for $1.1<\nu<1.4$, and in the neighborhood of $\nu=3$ a ferromagnetic phase is expected. A completely different approach is given in a recent work of Garanin *et al.*[13] Using calculations of spin-wave (SW) dynamics in magnetic particles, they have shown that in large enough particles, which reside in an unstable state, internal SW processes can lead to the nonexponential relaxation of magnetization and finally to magnetization reversal. However, in this model the relaxation take place by a change of the direction of magnetization, i.e., by a change of the sign of the normalized magnetization from $+m$ to $-m$ (m is the particle's magnetization), while the initial region of relaxation exhibits nonmonotonic behavior. We did not observe such features in our study of $La_{1-x}MnO_3$ nanoparticles. Instead, magnetization of 20 nm $La_{1-x}MnO_3$ nanoparticles was changed step by step after successive quick coolings while the relaxation observed was relatively weak.

An interesting model, which may provide a clue to the physics of diamagnetism and negative magnetization in $La_{1-x}MnO_3$, was recently proposed by Bulyzhenkov *et al.*[14] They showed that the Ginzburg-Landau bulk magnetization of itinerant electrons coupled to localized magnetic moments can provide a negative field in the Weiss model and can be negative or positive depending on the sample history. However, this model requires a prevailing paramagnetic positive susceptibility for the whole magnetic system, in contradiction to our experimental results, which exhibit a negative diamagnetic (DIA) susceptibility in a wide temperature range up to room temperature (RT). It appears that none of the above-suggested models is adequate for the 20 nm $La_{1-x}MnO_3$ nanoparticle system and many open questions regarding the observed strong DIA response are waiting for conclusive answers.

We have reported recently[11] on a study of electron-doped $Sm_{0.1}Ca_{0.84}Sr_{0.06}MnO_3$ (SCSMO) polycrystalline sample that exhibits a magnetic phase separation (PS) below $T_C \approx 105$ K, involving FM and AFM phases. It was found that, following a number of quick coolings (QCs), SCSMO placed in a capsule with a kerosene-oil mixture exhibits different metastable states with reduced ferromagnetism or DIA response, at $T<T_C$. It was suggested that the anomalous DIA behavior results from a specific coupling of the nanosize FM regions to the surrounding localized electron orbits, confined within the dislocation network formed by the numerous (7–8) cycles of QC.

The study of magnetic properties of self-doped $La_{1-x}MnO_3$ nanoparticles reported in this paper was inspired by these results.[11] Nanoparticles are well suited to further studies of the above peculiar effects, since they comprise all the ingredients obligatory for possible observation of a DIA response and negative ferromagnetism, such as a PS and nanocrystalline configuration for which the core-shell model[15,16] can be tested.

We define in this paper the term negative ferromagnetism as a magnetic state of material in which its temperature and field dependences of magnetization look similar to those of conventional ferromagnets, but the magnetization is antiparallel to the applied magnetic field.

II. EXPERIMENT

The $La_{1-x}MnO_3$ nanoparticles were prepared by well-known citrate method.[17] Lanthanum nitrate hexahydrate $La(NO_3)_3 \cdot 6H_2O$ 99.9% (Aldrich), manganese nitrate hexahydrate $Mn(NO_3)_2 \cdot 6H_2O$ 98% (Aldrich) and citric acid $HOC(CO_2H)(CH_2CO_2H)_2$ 99% (Aldrich) were taken in proportions to obtain a cation La to Mn ratio equal to 0.8. The molar amount of citric acid was equal to the sum of La and Mn cations. The ratio of La to Mn was chosen in order to reach maximal $T_C=252$ K as was found for self-doped $La_{1-x}MnO_3$ particles (see Ref. 18). The solution was continuously stirred at room temperature for 24 h and evaporated from open glass under stirring at 70 °C for 4 h until a gel was formed. Evaporation was prolonged in vacuum at room temperature for 4 h and at 70 °C overnight. Then the powder in the lowest layer was dried at 100 °C for 24 h, heated at a rate of 1 °C/min to the desired temperatures (700, 800, and 900 °C), and calcined at these temperatures for 8 h to get a series of $La_{1-x}MnO_3$ nanocrystalline powders with varying grain sizes.

The magnetic measurements were performed in the temperature range 4.2–300 K and magnetic fields up to 16 kOe, using a PAR (Model 4500) vibrating sample magnetometer (VSM). All measurements were carried out on cylinder-shaped samples having a diameter of 1 mm and height of 4.0 mm, prepared by compaction of the particle powder under pressure of 2 kbar. Measurements with the VSM were carried out on samples placed in a miniature CuBe container, serving as a sample holder, filled with silicon oil.[11] Additional measurements of the ac susceptibity were carried out using a quantum design physical property measurement system. In successive QCs, the following procedure was applied: A sample was placed in the container at room temperature and was then plunged into liquid helium (the speed of cooling was as high as 60–80 K/min). After measurements of the magnetization at 4.2 K the container with the sample was extracted from the cryostat and warmed back to RT for about 5 min. Then the procedure of QC was repeated until a state with large negative magnetization was obtained.

III. RESULTS AND DISCUSSION

The La and Mn contents were estimated by energy-dispersive x-ray spectroscopy (EDX) analysis with a JEOL JEM 5600 scanning electron microscope as the average of ten measurements performed at different points of the sample. The prepared powders were analyzed by the x-ray powder diffraction (XRD), transmission electron microscopy, and N_2-adsorption methods. The crystal structure of $La_{1-x}MnO_3$ nanoparticles was identified as a rhombohedral system of the $R\bar{3}C$ space group. The XRD pattern of the as-prepared sample (before heating) exhibits a fully amorphous phase. During calcinations, crystallization and grain growth of the perovskite manganite phase occurred. The amount of amorphous phase was still noticeable in the sample annealed at 700 °C (Fig. 1) and strongly decreased after higher-temperature (800 and 900 °C) annealing. Simultaneously, the manganese oxide Mn_3O_4 appeared as a para-

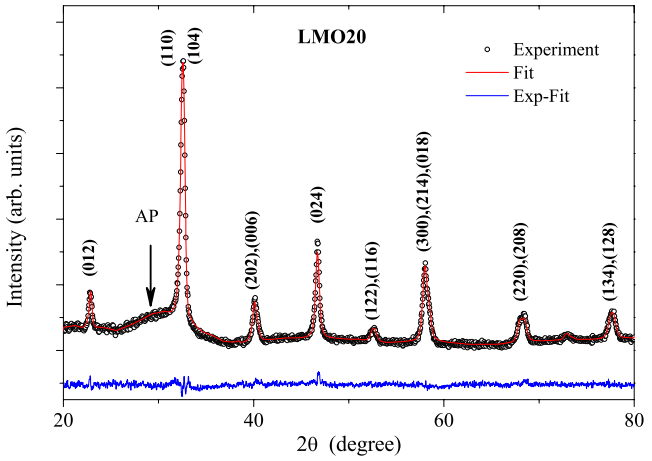

FIG. 1. (Color online) XRD spectra of LMO20 particles. The observed data points are indicated by open circles, the calculated and difference patterns are shown by solid lines. The main peaks are those of rhombohedral manganite. The halo from the amorphous phase (AP) is shown by an arrow.

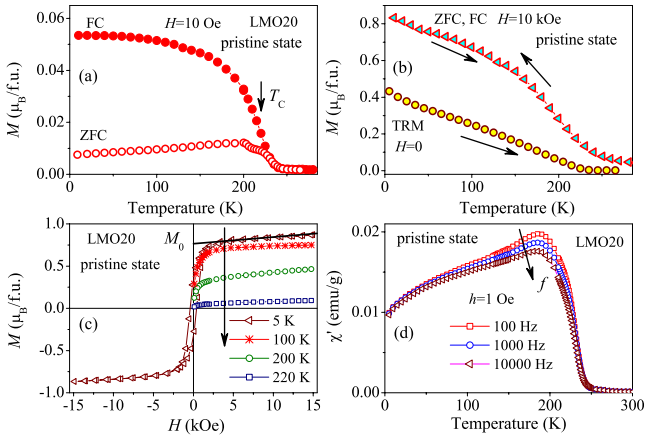

FIG. 2. (Color online) (a) Temperature dependence of ZFC and FC magnetization for LMO20 sample, in $H=10$ Oe and (b) in $H=10$ kOe. The TRM magnetization was recorded at heating in $H=0$ after cooling in $H=10$ kOe to 5 K and afterward reducing the field to zero. (c) Magnetization $M(H)$ of LMO20 sample in pristine state at $T \leq T_C$ after ZFC. (d) The in-phase component of ac susceptibility vs temperature of LMO20 sample at various frequencies. The probing field has amplitude of 1.0 Oe.

sitic phase in the sample annealed at 800 °C, and its amount increased with increasing temperature of the annealing. These observations are in reasonable agreement with results of thorough studies of the structural and magnetic properties of self-doped $La_{1-x}MnO_3$ nanoparticles.[18]

The average crystallite size was calculated using the Debye–Scherrer equation $\langle D \rangle = 0.9\lambda / b \cos\theta$, for the (024) reflection, where $\lambda = 1.540\,59$ Å for the $CuK_{\alpha 1}$ line, b is the full width at half maximum of the x-ray diffraction peak, and θ is the corresponding Bragg angle. It was found that $\langle D \rangle = 20$, 25, and 30 nm for samples annealed at 700, 800, and 900 °C, respectively. Since the anomalous DIA state was observed only for 20 nm $La_{1-x}MnO_3$ (LMO20) particles, we focus here on results obtained for this sample. The Rietveld refinement shows that the La to Mn ratio for the LMO20 sample (0.88) differs from the EDX data (La:Mn≈0.81). Previous studies[18] of $La_{1-x}MnO_3$ particles of 27–44 nm in size have revealed segregation of different phases instead of homogeneous sample composition and high value of $T_C > 200$ K for all samples. Dezanneau *et al.*[18] have shown that for La:Mn<0.9, the structure is no longer stable and separates into a vacancy-doped $La_{0.9}MnO_3$ phase and a parasitic Mn_3O_4 phase. Such a phase separation to an amorphous and a perovskite phase (LMO20 case) and to a perovskite and a Mn_3O_4 phase for 25 nm (LMO25) and 30 nm (LMO30) samples may lead to significant difference in the evaluation of the La to Mn ratios by different methods.

The measurements of the magnetization $M(T)$ of the LMO20 sample were performed according to the following procedure. The sample was cooled down in zero magnetic field to $T=5$ K and the magnetization was measured upon heating (ZFC curve) and immediately thereafter upon cooling (FC curve) under $H=10$ Oe, Fig. 2(a). The Curie temperature of the Mn spin sublattice, determined by the maximum slope in the $M_{FC}(T)$ dependence, is equal to $T_C \approx 220$ K, while the form of the FC curve indicates a broad magnetic transition. The large difference observed between ZFC and FC curves in low magnetic field of $H=10$ Oe [Fig. 2(a)] is completely suppressed when a magnetic field of 10 kOe is applied [see Fig. 2(b)]. The thermoremanent magnetization (M_{TRM}) of LMO20 was measured in the following way: The sample was cooled down to $T=5$ K in $H=10$ kOe, then the magnetic field was switched off and after a waiting time of ~100 s the $M_{TRM}(T)$ was recorded [see Fig. 2(b)]. It was found that M_{TRM} decreases monotonically with increasing temperature and completely vanishes at about 235 K, and then the response of the sample to the magnetic field becomes independent of history and reversible.

Figure 2(c) shows the magnetization $M(H)$ of the LMO20 sample recorded at various temperatures, following ZFC. As seen in Fig. 2(c), the spontaneous magnetization M_0, obtained by a linear extrapolation of the high-field magnetization to $H=0$, approaches a value of $M_0 \approx 0.76\mu_B$/f.u. at $T=5$ K and decreases with increasing temperature. The coercive field H_C is equal to about 390 Oe at 5 K. The relative volume of the FM phase at 5 K was estimated from the M_0 value to be about 24%. The real part of the susceptibility, χ', of the LMO20 sample [Fig. 2(d)] exhibits a wide magnetic transition as well as a significant dependence on frequency. It is worth noting that all the curves of χ' for LMO20 samples exhibit maxima at $T_p \approx 188$ K. This behavior is rather surprising, since for interacting and noninteracting nanoparticles,[19,20] as well as for spin glasses,[21] the temperature of the peak of χ' increases with increasing frequency. On the other hand, the almost flat shape of χ' below the peak is reminiscent of that observed in a disordered ferromagnets.[22] The magnetic interactions in a nanosized ferromagnetic particle are inhomogeneuos and exhibit a smeared-out Curie temperature T_C [see Fig. 2(a)]. The variation of the magnetic interactions and T_C also resembles the behavior of disordered ferromagnets, which like spin glasses exhibit a variety of metastable states.[22]

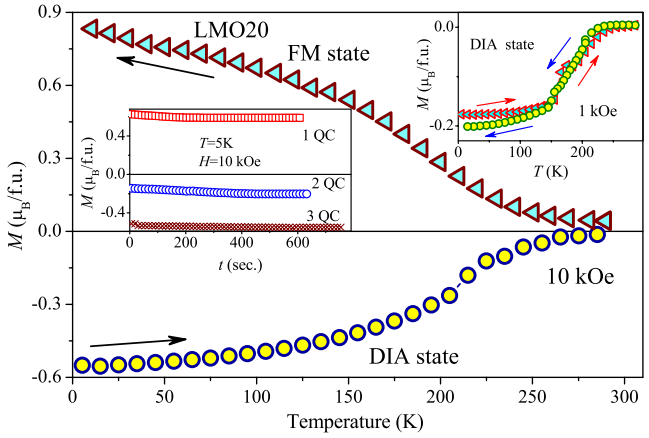

FIG. 3. (Color online) Magnetization $M(T)$ of LMO20 sample in metastable DIA state recorded at heating in $H=10$ kOe after three subsequent QCs in FC mode ($H=10$ kOe). For comparison, the FC magnetization recorded in the pristine state is also presented. Lower inset shows variation of magnetization with time after three successive quick coolings from RT to 5 K in $H=10$ kOe. After each QC the container with the LMO20 sample was taken out of the cryostat and heated up to RT, then the procedure of QC in the FC mode was repeated again. Upper inset shows magnetization $M(T)$ of LMO20 sample in an other metastable DIA state (obtained after successive QCs in $H=1$ kOe) recorded at heating and then at cooling in $H=1$ kOe.

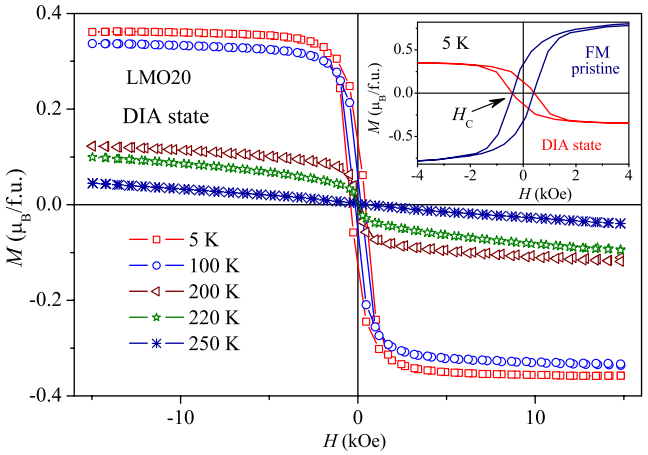

FIG. 4. (Color online) Magnetization $M(H)$ of LMO20 sample in metastable DIA state at various temperatures. Inset shows comparison between M vs H curves recorded at $T=5$ K in both pristine and metastable DIA states.

Further measurements of the magnetization of LMO20 were performed on samples placed in a container filled with silicon oil and quickly cooled from RT to $T=5$ K, at the rate of 80 K/min. under $H=10$ kOe. This procedure resulted in a metastable state with reduced magnetization, characterized by a relatively weak relaxation, even after the first QC (see lower inset in Fig. 3). After that, the container with the sample was removed from the cryostat, heated up to RT for about 5 min in a flow of warm air, and then QC again at the same FC mode. The second sequential QC cycle was found to be sufficient for reversing the magnetization (inset in Fig. 3, 2 QC). A higher value of the metastable negative magnetization was obtained after the third QC. The negative magnetization appears to be a mirror replica of the magnetization in the pristine state for a wide temperature range at $T<T_C$ and even at $T>T_C$ (see Fig. 3). T_C(DIA) as determined by the maximum in the derivative of the magnetization $dM(T)/dT$ is $\approx$215 K, close to the value of T_C obtained in the pristine state (see Fig. 2). It was found that the states of negative magnetization retain their write-in memory after heating up the sample to RT for several minutes (see upper inset in Fig. 3). This inset displays the temperature dependence of the magnetization in a DIA metastable state (obtained after several subsequent QCs in $H=1$ kOe), recorded at warming up to 285 K under $H=1$ kOe, and immediately after that recorded at cooling under the same magnetic field. Keeping the sample at RT for only a few hours resulted in erasing of the DIA memory and restoration of the pristine state. In this paper the name "pristine state" characterizes the state of the LMO20 sample in which its $M(T)$ and $M(H)$ dependences coincide with those presented in Fig. 2. Further measurements of the DIA states and negative magnetization were carried out under various FC fields, ranging from 100 Oe up to 10 kOe and in the ZFC mode as well. In the latter case an external magnetic field was applied at $T=5$ K in order to compare the DIA response for each QC. It appears from this study that a magnetic field is not a prerequisite for the creation of DIA metastable states.

Figure 4 presents $M(H)$ curves of the LMO20 sample in the DIA state at various temperatures, observed after QC thermal cycling. The following features are noticeable. (i) A linear DIA field-dependent response is observed for $T>220$ K up to $H=15$ kOe. One finds the dc susceptibility $\chi_{\text{dia}}\approx -7\times10^{-5}$ emu g^{-1} Oe^{-1} at $T=250$ K. At $T\leq220$ K there is an additiononal high-permeability DIA contribution superimposed on the susceptibility. (ii) The H_C increases with decreasing temperature and reaches the value of about 400 Oe at $T=5$ K (see inset in Fig. 4).

One notes that the DIA phase observed in a SCSMO polycrystal[11] and compacted LMO20 particles occurs only under very critical conditions, namely, quick cooling ($\sim$60–80 K/min) of the sample, which is placed in a capsule filled with some liquid media. It was found that QCs without the liquid media do not lead to the appearance of the DIA effect. Moreover, it is worth noting that LMO particles with greater size and greater volume of the FM phase ($\sim$74% and 93% for 25 nm and 30 nm LMO particles, respectively) do not exhibit the DIA phase.

Let us compare the magnetic properties of the two compounds in which we observed the striking DIA effect: polycrystalline SCSMO (Ref. 11) and LMO20 particles. Both compounds in the pristine state exhibit features reminiscent of a cluster glass: a gap between ZFC and FC magnetizations and the frequency dependence of χ', which maximizes at a hump below T_C. Moreover, the relative amount of the FM phase is practically the same ($\sim$25%) for both samples. It was previously reported[11] that SCSMO exhibits a magnetic PS below $T_C\approx100$ K, consisting of FM domains embedded in an AFM matrix. Congenital PS in the case of the LMO20

sample stems from the core-shell structure proposed for different manganite particles.[15,16,23] In this model, the inner part of the particle, i.e., the core, has the same properties as the bulk material, whereas the outer layer, namely, a shell, contains most of the oxygen faults and vacancies in the crystallographic structure, leading to a magnetically dead layer. We believe that only the inner core of the LMO20 particles consists of a FM phase, below T_C, whereas the outer shell is presumably not FM. Further studies are needed to clarify the spin configuration of the outer shell in the pristine state, whether it is paramagnetic or AFM in nature. Nevertheless, it appears that the interplay between the two magnetically different phases plays the key role in the DIA effect. As was noted already, larger $La_{1-x}MnO_3$ nanoparticles of 25 and 30 nm do not exhibit the phenomenon of metastable diamagnetism. We believe the reason for the absence of this effect in larger particles lies in the necessity of a fine balance between the volumes of the two coexisting phases: FM cores and DIA shell. In the cases of LMO25 and LMO30, the ferromagnetic phase (cores) occupies almost the whole volume of the nanoparticles at low temperatures, and the outer shell is much thinner than that for the LMO20 sample. Consequently, we may suggest that the field of the DIA matrix in the LMO25 and LMO30 samples is too weak to align the magnetic moment of the FM cores opposite to the magnetic field.

It has been suggested[11] that the DIA behavior of SCSMO may be related to a metastable nanocrystalline configuration resulting in a localized wave function of electrons. The localized orbiting electrons may form a DIA matrix and give rise to the linear DIA response at $T > T_C$. The highly enhanced negative magnetization observed at $T < T_C$ may occur concurrently with PS, when the FM clusters couple via a specific exhange interaction to the DIA matrix, giving rise to the appearance of negative ferromagnetism. The observation of similar effects in LMO20 nanoparticles may support the above scenario. The characteristic DIA nature of the so-called DIA matrix was established by our magnetization measurements of the metastable magnetization above T_C (Fig. 4). As mentioned already, the existence of local, atomic-scale, nondissipative currents may be a clue to the above observations of metastable diamagnetism. One may also consider such current paths as local atomic-scale superconductivity.

The observations of metastable diamagnetism in two different compounds, LMO20 particles and a SCSMO polycrystal, raise some open questions concerning the conditions of the preparation method, the morphology of the sample, the microstructure, and the cycles of QC. There is no definite answer, in our opinion, but at least one can compare the crystallographic and magnetic properties of the two compounds exhibiting metastable diamagnetism and negative magnetization: (i) in both samples a PS is a distinctive property; (ii) the samples are characterized by a similar cluster-glass-like behavior; (iii) the same relative volume ($\sim 25\%$) of the FM phase was observed in both of them; (iv) the DIA state was achievable only after several QCs in a container filled with liquid medium (thermal contact and the source of extra stress during QC).

IV. CONCLUSIONS

In conclusion, this study reports the observation of metastable DIA states and negative ferromagnetism in compacted 20 nm $La_{1-x}MnO_3$ particles. It was found that the particles possess only a small volume of FM phase, about 24% at 5 K, and exhibit a magnetic transition at $T_C \approx 220$ K. Sequential QCs of the sample held in a capsule filled with silicon oil result in metastable states with reduced magnetization, and finally in a negative magnetization. The state with the largest negative magnetization was found to be stable at $T > T_C$, becoming erasable only after a few hours storage of the sample at room temperature. In the case of LMO20 particles, the FM properties of the sample are related directly to the inner FM core of the particles, their magnetic anisotropy, and the magnetic interaction between neighboring particles. The outer shell of the particles in the pristine state may not display magnetic ordering, and supposedly it is paramagnetic.[15,16,24] Being strained by the QC cycles, the shell, according to the present scenario, becomes DIA and retains this slowly relaxing property well above T_C. A specific coupling between the two magnetically different phases may play the key role in the DIA effect. The nature of the diamagnetism of the shell matrix, whether it results from local atomic-scale nondissipative superconductinglike currents or is a property of the strained material, is not clear at this stage of the studies. Among the samples with average crystallite size of 20, 25, and 30 nm, only the 20 nm particles exhibit DIA effects, meaning that the core-shell structure configuration also seems to be critical. Further investigations of the effect of particle size and of the variation in chemical composition may provide better insight into the underlying physics.

ACKNOWLEDGMENTS

The authors thank D. I. Khomskii and K. Kikoin for useful discussions. This work was supported in part by the Polish State Committee for Scientific Research under Research Project No. 1 P03B 123 30 and by the Israeli Science Foundation, grant 391/07.

*Corresponding author: markoviv@bgu.ac.il

[1] H. C. Nguyen and J. B. Goodenough, Phys. Rev. B **52**, 324 (1995); J.-Q. Yan, J.-S. Zhou, and J. B. Goodenough, *ibid.* **72**, 094412 (2005).

[2] Y. Ren, T. T. M. Palstra, D. I. Khomskii, E. Pellegrin, A. A. Nugroho, A. A. Menovsky, and G. A. Sawatsky, Nature (London) **396**, 441 (1998).

[3] M. Moiallem-Bahout, O. Peña, D. Gutierrez, P. Duran, and C. Moure, Solid State Commun. **122**, 561 (2002); O. Peña, M. Bahout, D. Gutierrez, P. Duran, and C. Moure, Solid State Sci.

5, 1217 (2003).
[4] C. A. Nordman, V. S. Achutharaman, V. A. Vas'ko, P. A. Kraus, A. R. Ruosi, A. M. Kadin, and A. M. Goldman, Phys. Rev. B **54**, 9023 (1996).
[5] G. J. Snyder, C. H. Booth, F. Bridges, R. Hiskes, S. DiCarolis, M. R. Beasley, and T. H. Geballe, Phys. Rev. B **55**, 6453 (1997).
[6] J. Hemberger, S. Lobina, H.-A. Krug von Nidda, N. Tristan, V. Yu. Ivanov, A. A. Mukhin, A. M. Balbashov, and A. Loidl, Phys. Rev. B **70**, 024414 (2004).
[7] F. Bartolomé, J. Bartolomé, and J. Campo, Physica B **312-313**, 769 (2002); F. Bartolomé, J. Herrero-Albillos, L. M. Garcia, J. Bartolomé, N. Jaouen, and A. Rogalev, J. Appl. Phys. **97**, 10A503 (2005).
[8] I. O. Troyanchuk, V. A. Khomchenko, S. N. Pastushonok, O. A. Novitsky, V. I. Pavlov, and H. Szymczak, J. Magn. Magn. Mater. **303**, 111 (2006).
[9] I. Dzyaloshinskii, J. Phys. Chem. Solids **4**, 241 (1958).
[10] T. Moriya, Phys. Rev. **120**, 91 (1961).
[11] V. Markovich, I. Fita, R. Puzniak, C. Martin, K. Kikoin, A. Wisniewski, S. Hebert, A. Maignan, and G. Gorodetsky, Phys. Rev. B **74**, 174408 (2006).
[12] D. C. Mattis, Physica B **384**, 239 (2006).
[13] D. A. Garanin, H. Kachkachi, and L. Reynaud, arXiv:cond-mat/0609074 (unpublished).
[14] I. Bulyzhenkov, A. M. Lamarche, and G. Lamarche, Phys. Rev. B **72**, 155203 (2005).
[15] T. Zhu, B. G. Shen, J. R. Sun, H. W. Zhao, and W. S. Zhan, Appl. Phys. Lett. **78**, 3863 (2001).
[16] M. A. López-Quintela, L. E. Hueso, J. Rivas, and F. Rivadulla, Nanotechnology **14**, 212 (2003).
[17] M. S. G. Baythoun and F. R. J. Sale, Mater. Sci. **17**, 2757 (1982).
[18] G. Dezanneau, M. Audier, H. Vincent, C. Meneghini, and E. Djurado, Phys. Rev. B **69**, 014412 (2004); G. Dezanneau, A. Sin, H. Roussel, M. Audier, and H. Vincent, J. Solid State Chem. **173**, 216 (2003); G. Dezanneau, A. Sin, H. Roussel, M. Audier, and H. Vincent, Solid State Commun. **121**, 133 (2002).
[19] T. Jonsson, P. Nordblad, and P. Svedlindh, Phys. Rev. B **57**, 497 (1998).
[20] S. D. Tiwari and K. P. Rajeev, Phys. Rev. B **72**, 104433 (2005).
[21] J. A. Mydosh, *Spin Glasses* (Taylor and Francis, London, 1993).
[22] V. Dupuis, E. Vincent, M. Alba, and J. Hammann, Eur. Phys. J. B **29**, 19 (2002); E. Vincent, V. Dupuis, M. Alba, J. Hammann, and J.-P. Bouchaud, Europhys. Lett. **50**, 674 (2000).
[23] N. Zhang, W. Ding, W. Zhong, D. Xing, and Y. Du, Phys. Rev. B **56**, 8138 (1997).
[24] M. Bibes, L. Barcells, J. Fontcuberta, M. Wojcik, S. Nadolski, and E. Jedryka, Appl. Phys. Lett. **82**, 928 (2003).